Electrochemical and Solid-State Letters, **9** (9) A418-A422 (2006)
1099-0062/2006/9(9)/A418/5/$20.00 © The Electrochemical Society

Temperature-Driven Water Transport Through Membrane Electrode Assembly of Proton Exchange Membrane Fuel Cells

Rachid Zaffou,[a,*,z] Jung S. Yi,[b,] H. Russell Kunz,[a,**] and James M. Fenton[c,**]**

[a]*Department of Chemical Engineering, University of Connecticut, Storrs, Connecticut 06269, USA*
[b]*Arkema Incorporated, King of Prussia, Pennsylvania 19406, USA*
[c]*Florida Solar Energy Center, University of Central Florida, Florida 32922, USA*

A quantitative investigation has been carried out to examine the effect of through-plane temperature difference on water transport across the membrane electrode assembly (MEA) of a proton exchange membrane (PEM) fuel cell. The presence of a temperature difference across the cell was found to cause a significant amount of water to transport through the MEA in the direction towards the colder side; the water transport rate increased with temperature and temperature gradient. This study reveals the importance of thermo-osmosis in PEM fuel cells (PEMFCs) and the need to consider the through-plane temperature profile in water management design and operation in PEMFCs.
 [DOI: 10.1149/1.2218306]

Manuscript submitted February 7, 2006; revised manuscript received May 23, 2006. Available electronically June 27, 2006.

Adequate water management is critical for proton exchange membrane fuel cell (PEMFC) performance and durability.[1-5] Excess water can cause performance degradation due to liquid water flooding in various layers of the fuel cell. An inadequate water balance in the cell can lead to membrane dehydration, which lowers performance as well as the lifetime of the cell. Therefore, understanding water movement within the cell is an important aspect for PEMFC development.

Water is believed to be transported across the membrane of an operating PEMFC in various modes. One of these is electro-osmosis, which involves drag of water molecules by protons from the anode to the cathode side of the membrane upon passage of current. Meanwhile, accumulation of water in the cathode side, not only by electro-osmosis, but also by water generation in the cathode electrode, causes a gradient in the chemical potential of water, which drives water back to the anode.

Recently, it has been discovered that a through-plane temperature difference across an operating PEMFC also causes water to move across a Gore membrane electrode assembly (MEA).[6] In this study, we have demonstrated, for the first time, experimental evidences of the presence of thermo-osmotic water transport across a MEA in a PEMFC.

Approach

Studying water transport across the MEA of an operating PEMFC requires water balance measurements within the system at known MEA operating conditions. Such measurements raise concerns of methodology due to the complexity of water distribution within the cell. Typically, undersaturated reactant gases are introduced into the cathode flow channels of the fuel cell. Thus, when the water vapor from the water generated in the cathode electrode is mixed with the reactant gas stream, the humidity level of these gases increases as they travel along the flow channels. Based on various PEMFC water management schemes, the anode and the cathode reactant flows are configured to distribute water internally within the cell more uniformly to maintain adequate humidification of the membrane and the electrodes as well as to prevent liquid water flooding in the various layers of the PEMFC assembly. Under these conditions, the water vapor partial pressure becomes the primary driving force for water distribution through the membrane. Due to this dominant effect of vapor partial pressure, studying other water transport phenomena occurring through the membrane during the operation of the cell, which may be equally important, may not be feasible. In addition, water vapor partial pressure of the reactant gas streams changes as the gases travel along the flow channels.[1,2,4,5,7] Therefore, the humidity level of the cathode and the anode reactant gas streams, which need to be systematically varied to investigate other independent parameters that may affect the transport of water through the MEA, becomes impossible to identify.

Another challenging aspect in water balance measurements is related to low temperature operation. Mass-transport limitations associated with liquid water flooding become more apparent especially at low temperatures, causing loss in cell performance and possibly cell failure.[8-10] Under such conditions, an adequate water management system becomes particularly crucial in maintaining stable cell performance and, hence, ensuring proper water balance measurements.

To circumvent these difficulties, the water balance measurements of an operating PEMFC were performed using an intracell water-exchange scheme, which is used in the UTC fuel cells PEMFC stack designs.[4,11] This design utilizes water transport plates (WTPs), which are carbon plates with fine pores filled with liquid water. Besides providing flow channels for reactant gases, WTPs allow liquid water to circulate through the cell via liquid water channels situated in the back of each WTP. A pressure difference that is maintained between the gas channels and the water channels in the WTPs ensures that liquid water accumulated in the reactant flow channels is transported through the WTP and out of the cell. In addition to its capability to remove liquid water from the cell, the WTPs can internally provide water to the cell when the supplied gas is undersaturated, which helps to maintain fully humidified conditions inside the cell and to prevent membrane dehydration. This feature allows the gas streams to maintain fully saturated conditions within the cell, eliminating the vapor pressure-driven water flow through the MEA. Also, because of its capability to remove water in the liquid phase, the intracell water-exchange fuel cell scheme remains effective in sustaining stable cell performance under a wide range of operating temperatures.[10] This allows water balance measurements to be properly conducted in an operating PEMFC at various cell temperatures.

With the intracell water-exchange fuel cell design, two different modes of operation were used to investigate the significance of thermo-osmosis in a MEA. First, while supplying vapor-saturated reactant gases on both sides of the MEA and maintaining an electrical load in the cell, the relative significance of the thermal osmosis on the water movement in operating fuel cell conditions was examined. In this experimental configuration, other effects induced by factors such as water generation, gas flow rates, and the vapor pressure, which are set by the temperature of the gas stream, are also included along with the effect of the material properties of the adjunct layers that may have an effect on the water transport rate and its direction through the MEA. To confirm the phenomenon more clearly, a second mode of operation was also used. In this phase of the experiments, the cell configuration was changed to allow for the MEA to be equilibrated with liquid water in the anode and in the cathode WTPs. In this simplified liquid-water-filled configuration,

* Electrochemical Society Student Member.
** Electrochemical Society Active Member.
z E-mail: rachid@engr.uconn.edu

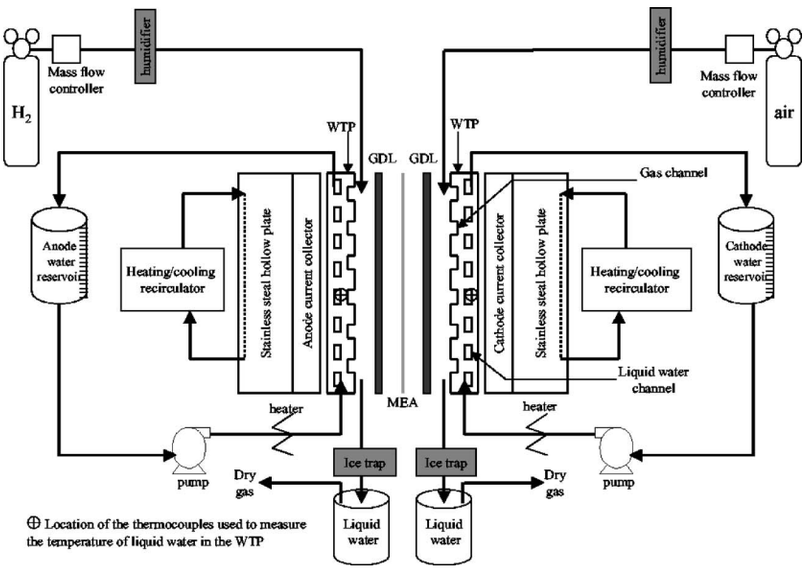

Figure 1. Schematic diagram of the experimental setup.

all other driving forces associated with normal cell operation are eliminated except for the temperature difference; it remained the only source that can affect water flow through the MEA. Therefore, an experimental demonstration of the effect of the thermo-osmosis phenomenon in the MEA was achieved. The details of the experimental apparatus and the operating conditions used in this study are discussed in the following section.

Experimental

Figure 1 illustrates the experimental setup used for this study. The MEA, together with the gas diffusion layers, were sandwiched between two WTPs, which, in turn, were sandwiched between two gold-coated stainless steel plates for current collection and to provide the cell assembly the axial load compression. The temperature of the cell was maintained by heating liquid water from the water reservoirs entering the WTPs. An additional heating/cooling source was provided by a heating/cooling recirculator that circulated ethylene glycol through stainless steel hollow plates attached to each side of the cell. Additional thermocouples were placed at the gas streams exiting the ice traps and at all gas streams entering and exiting the cell. The temperature of each side of the cell, which was monitored through a thermocouple placed in the liquid water channel in the anode and the cathode WTP (Fig. 1), was achieved by setting the temperature of all streams entering the cell to the desired temperature. Temperatures of the anode and the cathode entering streams were independently controlled. Insulating materials were installed around the cell to help maintain stable and uniform cell temperatures.

In all experiments, the cell configuration remained unchanged. A Gore 5510 MEA (Gore Fuel Cell Technologies) was used that consists of a 15 μm thick reinforced perfluorosulfonic acid membrane coated on both sides with 0.4 mg_{Pt}/cm^2 (Pt/C) catalyst. The total cell active area was 25 cm^2. A gas diffusion layer consisting of 254 μm thick Toray paper (SGL, 10BB, Carbon Group, Wiesbaden, Germany) was used at the anode. A 254 μm total thickness in-house gas diffusion layer made of Toray paper with microporous layer containing Vulcan XC-72R (Cabot Corporation, Bellerica, MA) and polytetrafluoroethylene was used at the cathode.[12] The type of the gas diffusion layer used at the cathode was selected to ensure proper water management during operation, which is important in maintaining stable cell performance during the experiments.

As seen in Fig. 1, water reservoirs, which were open to the atmosphere, were connected to the inlet and exit ports of each WTP. During operation, the pump, which connects the water reservoir to the WTP, allowed continuous circulation of water through the WTPs. The excess water at each side of the cell was removed through the WTPs and out of the cell to be collected in the water reservoirs. A calibrated measurement scale placed on the water reservoirs allowed the monitoring of water movement inside the cell as a function of time. Reactant gases used in this study were 100% humidified. The amount of water vapor entering the cell was calculated from the dew point temperature of each reactant inlet stream. The cathode and the anode effluents were passed through an ice trap to condense water vapor exiting the cell. The temperature of the gas streams exiting the ice trap was used to calculate the remaining water vapor entrained in the ice-trap exit stream.

In all experiments, water balance measurements were carried out after reaching stable cell performance at the desired temperature as indicated by the thermocouple placed in the liquid water channel of each WTP. This was achieved by adjusting the temperature of the humidifiers, the temperature of liquid water entering the WTPs, and the temperature of the hollow stainless steel plates at each side of the cell to the desired temperature. After the current load was applied, the cell voltage was allowed to stabilize. During each experiment, the water level in the anode and the cathode water reservoirs was recorded for a period of 2 h; all readings were taken at a nearly equivalent time period. Cell voltage and temperatures of all streams exiting and entering the cell were also recorded as a function of time throughout each experiment. The condensed liquid water in the ice trap from the cathode and the anode exiting streams was weighed at the end of each test. The liquid water level in each reservoir was readjusted to become equal prior to each test. The water balance was evaluated at 0.4 A/cm^2 cell current density under fixed flow of hydrogen (0.2 L/min) and air (1 L/min). Initially, the effect of temperature on water transport across the membrane was identified; the experiments were carried out by performing total-cell water balance measurements under isothermal cell conditions (55, 60, 65, 70, and 75°C). These temperatures were attained as described earlier. Upon applying the current load, the heat generated in the cell caused some fluctuations of the temperatures, as detected by the thermocouples, especially when operating the cell at lower temperatures. In these cases, the temperature of the hollow stainless steel plates was readjusted and the cell was allowed to equilibrate before the measurements were initiated. Although some variations in the cell temperature were present when attempting to operate the cell under isothermal conditions, the effects of these fluctuations on water transport across the MEA are believed to be insignificant, especially when compared with the cases where the cell was subjected to a temperature difference. The effect of temperature difference was then addressed; the water balance measurements were conducted

Table I. The values of the net water flow rate m^a_{mem} and m^c_{mem} as a function of temperature of liquid water in the cathode and the anode WTP. All data were acquired in an operating PEMFC (i = 400 mA/cm^2, active area = 25 cm^2, near ambient pressure, 100% relative humidity (RH), H_2 (0.2 L/min), air (1 L/min), P_{vacuum} = −17 kPa). m^a_{mem} and m^c_{mem} were obtained according to Eq. 1 and 2, respectively.

Temperature of liquid water in $WTP_{cathode}$ (°C)	Temperature of liquid water in WTP_{anode} (°C)	Cell voltage (V)	m^a_{mem} (g/min)	m^c_{mem} (g/min)	Error[a] (%)
60	60	0.688	−0.0323	−0.0388	12
			−0.0243	−0.0308	12
	57	0.688	−0.0599	−0.0575	−4
			−0.0502	−0.0598	17
	55	0.680	−0.0633	−0.0664	6
			−0.0626	−0.0696	13
	50	0.686	−0.1090	−0.1101	2
			−0.1105	−0.1077	−5
65	65	0.671	0.0042	0.0042	0
			−0.0061	−0.0075	2
	62	0.689	−0.0551	−0.0639	16
			−0.0546	−0.0639	17
	60	0.690	−0.0714	−0.0808	17
			−0.0767	−0.0772	1
	55	0.690	−0.1322	−0.1397	13
			−0.1117	−0.1171	10
70	70	0.675	0.0034	0.0064	−5
			0.0053	0.0053	0
	67	0.684	−0.0680	−0.0659	−4
			n/a[b]	n/a	n/a
	65	0.684	−0.0831	−0.0853	4
			−0.0788	−0.0747	−7
	60	0.692	−0.1369	−0.1422	9
			−0.1453	−0.1466	2
75	75	0.682	0.0575	0.0573	0
			n/a	n/a	n/a
	72	0.680	−0.0603	−0.0647	8
			n/a	n/a	n/a
	70	0.684	−0.1159	−0.1153	−1
			n/a	n/a	n/a
	65	0.682	−0.1674	−0.1602	−13
			−0.1694	−0.1648	−8

[a] Error = $(-m^c_{mem} + m^a_{mem})/m_{ger} \times 100$
[b] n/a: not available

while maintaining a temperature differential across the cell. The experimental conditions used for this investigation are listed in Table I. Most of the experiments discussed above were repeated twice as reported in the table.

While keeping the cell assembly intact, the cathode and the anode of the cell were purged with nitrogen to remove reactant gases that may still be present. The pumps connecting the water reservoirs were removed and the reactant streams were disconnected from the cell. Using liquid-water pumps, liquid water was forced into the flow fields of the WTPs, causing liquid water to occupy the entire cell. The pumps were then disconnected, followed by applying vacuum (−30 in. Hg) at the top of the liquid-water reservoirs. Vacuum was removed when gas bubbles leaving the cell through the water reservoirs were no longer observed. Liquid water in the cell was then allowed to equilibrate for a few hours. Prior to each test, the water levels in the anode and in the cathode water reservoirs, which remained open to the atmosphere, were adjusted to about 12 in. With no entering or exiting streams (closed system), the cell was exposed to a temperature difference, which was achieved by adjusting the temperature of the hollow stainless steel plates using the external heating/cooling recirculator. The water level in the anode and the cathode water reservoirs was again monitored with time

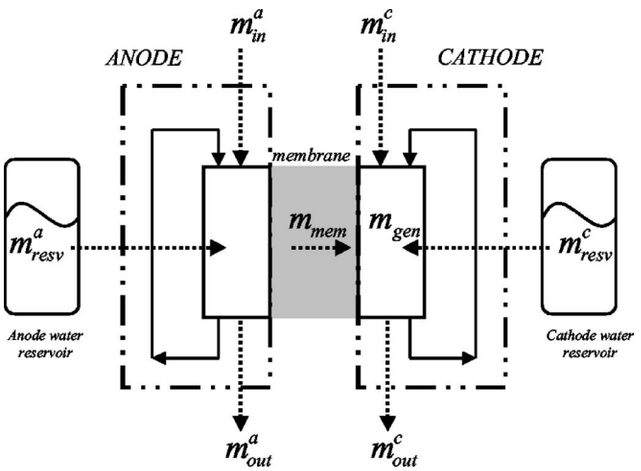

Figure 2. Schematic representation of the various water flows entering and exiting the anode and the cathode side of the cell, including the water generated in the cathode and the water flow through the membrane (m_{mem}) during the operation of the cell. m_{in} is total water flow rate entering the cell with the reactant gases, m_{out} is total water flow rate exiting the cell with reactant streams, m_{resv} is total water flow rate supplied by liquid water reservoir, m_{mem} is total water flow rate across the membrane ($m_{mem} = m^c_{mem}$). *a* is anode, and *c* is cathode.

with and without the introduction of temperature difference across the cell. These experiments were performed maintaining the temperature in the water channel of the cathode WTP 0, 3, 5, and 10°C higher than that of the anode WTP. Three cathode WTP temperatures were investigated (55, 60, and 65°C). During this part of the experiment, the cell was held at open circuit.

Results and Discussion

As discussed earlier, measurements of water flow entering and exiting the cell were carefully carried out for each operating condition. Figure 2 illustrates the various water flows entering and exiting the anode and the cathode side of the cell, including the water flow generated during the cell operation. The mass balance of water on the anode side of the cell results in the net water flow rate across the membrane, as shown in Eq. 1. The same information can be obtained from the mass balance of water on the cathode side of the cell, as expressed in Eq. 2.

$$m^a_m = m^a_{in} + m^a_{resv} - m^a_{out} \quad [1]$$

$$m^c_m = m^c_{out} - m^c_{in} - m^c_{resv} - m_{gen} \quad [2]$$

The values of the net water flow rate across the membrane m^a_{mem} and m^c_{mem} obtained from two different sets of measurements should yield identical results. However, due to experimental inaccuracies, these values may differ. This difference can be used as an indication of the accuracy of the experimental measurements. Table I shows the operating conditions, the measured cell potential, and the measured total water flow rates through membrane, m^a_{mem} and m^c_{mem} calculated according to Eq. 1 and 2, respectively. The magnitude of the deviation in the measurements was estimated to be 17% or less of the water generation rate. Inaccuracy from dew point measurements in the entering and exiting water streams and the evaporative loss in the water reservoirs during testing may be the cause of the observed discrepancies. Due to the low permeation rate of hydrogen through the MEA, the water generated due to hydrogen crossover was ignored. However, this additional water may have contributed to the discrepancies observed, especially in the cases where the measured cathode net water flow was higher than that of the anode. Due to the presence of a temperature difference across the cell, a significant flux in the direction towards the cold side of the cell, that is the

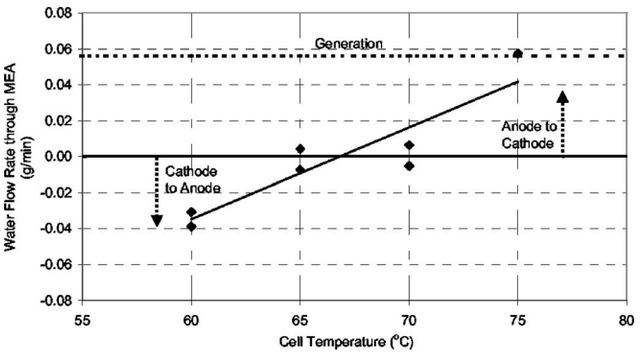

Figure 3. Effect of temperature on water distribution across the MEA of an operating PEMFC [i = 400 mA/cm^2, active area = 25 cm^2, near ambient pressure, 100% RH, H_2 (0.2 L/min)/air (1 L/min), P_{vacuum} = −17 kPa].

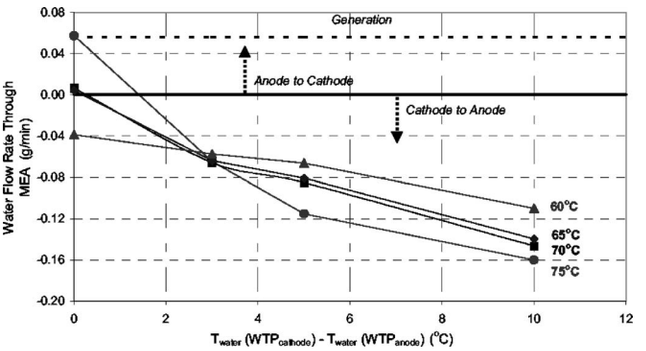

Figure 4. Effect of through-plane temperature difference on water distribution across the MEA of an operating PEMFC. 60, 65, 70, and 75°C represent the temperatures of liquid water at the cathode WTP [i = 400 mA/cm^2, active area = 25 cm^2, near ambient pressure, 100% RH, H_2 (0.2 L/min)/air (1 L/min), P_{vacuum} = −17 kPa].

anode in this study, is observed. As a result, the anode may experience some liquid-water flooding, especially at lower temperatures. Under these conditions, due to the fast diffusion of hydrogen, the anode flooding may have no affect on the cell performance, and therefore, it will not be detected. In contrary, the cell performance is very sensitive to cathode flooding and any accumulation of water at the cathode electrode will directly affect the cell performance and hence it will be detected, which will then require adjustment of the operating conditions. For these reasons, and for further analysis, the estimated total water flow rates at the cathode side were used.

As mentioned in the experimental section, the water balance measurements were first performed while maintaining uniform temperature across the cell. Then the temperature of the anode side of the cell was lowered while holding the temperature of the cathode side constant, thereby generating the desired temperature difference between the anode and the cathode side of the cell. First, the results of the effect of temperature on the net water transport rate across the membrane are shown in Fig. 3. This data represents the results of two sets of experiments. Positive flow rates represent water movement across the membrane from the anode to the cathode side of the cell. The water generation rate was also plotted in Fig. 3 to illustrate the relative magnitude of the measured water flow rate across the membrane. Water transport in a PEMFC is dependent not only on the operating conditions, but also on the material properties of the components used in the cell. Therefore, the results reported in Fig. 3 are specific to the cell design used in this study, and the conclusions drawn are used as a baseline to later identify how water distribution across a membrane can be affected by the presence of a temperature difference across the cell. However, the results from this specific case demonstrate that the cell temperature can be an important parameter to determine the water transport properties across the membrane. At 60°C, the water flows through the membrane in the direction towards the anode side of the cell at a rate similar to the water generation rate at a current load of 400 mA/cm^2. Increasing temperature causes less water to be transported through the membrane. Then, at 75°C, the water flow rate is seen to move through the membrane from the anode side to the cathode side with a rate similar to the water generation at the cathode at the applied current density.

Figure 4 shows the water flow rate across the membrane of a PEMFC operating under the effect of a through-plane temperature differential. The data are presented as an average of the calculated net water flow from two sets of experiments. It is seen that water flows through the membrane in the direction towards the colder side of the cell. The rate can be significantly higher than the water generation rate for the temperature applied in this study. As can be observed, at a fixed temperature difference, the higher the set temperature, the higher the water flow rate in the direction towards the cold side of the cell. The temperature differences reported in Fig. 4 represent the difference in temperature of liquid water in the WTP between the cathode and the anode side of the cell. In a typical PEMFC, factors such as the heat generated especially at the cathode, the energy exchange due to the evaporation or condensation of water, the difference in thermal conductivities of the various cell components, and the cooling techniques used during operation can induce a through-plane temperature difference within the cell. This temperature difference can be further magnified in PEMFC stack particularly during transient operation.[13-15] Consequently, the magnitude of the temperature difference between each side of a single-cell package investigated in this study is considered to be realistic. Therefore, it is clear that the presence of a temperature difference across an operating PEMFC can have a strong impact on water distribution inside the cell. Also, based on the value of the electro-osmotic drag coefficient for Nafion membrane equilibrated with water vapor reported in the literature,[16] the amount of water dragged due to the passage of protons across the membrane at a current density of 0.4 A/cm^2 results in water flow rates comparable to what was measured in the case of the temperature-driven water transport (Table I). Through-plane temperature difference can generate a strong driving force for water transport across the membrane during the operation of a PEMFC.

Further measurements of net water transport across a PEMFC were performed. As previously mentioned, the cell was held in a closed system with no entering or exiting streams while maintaining liquid water inside the flow channels in the WTPs. The anode and cathode water reservoirs connected to the WTPs served as liquid-water level indicators to monitor water movement across the cell (Fig. 1). The water was set to the same level in each water reservoir prior to each experiment. The amount of water transported across the cell is given in Fig. 5 as a function of the temperature difference. As can be seen in Fig. 5, the presence of the temperature difference across the cell generated liquid water movement in the direction towards the colder side of the cell, and the flow of water appeared to increase with temperature and with temperature difference. The qualitative comparison between the data collected from the earlier experiments shows a good agreement. However, the values for water flow rate shown in Fig. 4 are different from the ones presented in Fig. 5. This difference is believed to be due to the fact that the earlier experiments were performed under an operating PEMFC, which involves the supply of humidified reactant gases to the cell and the generation of heat due to the exothermic reaction that takes place in the cathode. These conditions may contribute to some variations in the actual temperature profile across the cell. Based on permeability values reported in the literature,[17] calculations were performed to estimate the pressure required to transport water across the MEA at rates comparable to what was observed with the presence of a temperature difference across the cell. To transport liquid water at flow rate similar to what was measured in the case of a

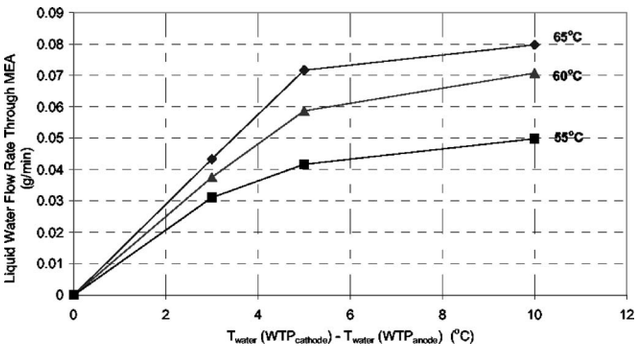

Figure 5. Effect of through-plane temperature difference on water distribution across the MEA of a PEMFC (flooded configuration). 55, 60, and 65°C represent the temperatures of liquid water at the cathode WTP.

flooded cell with a temperature difference of 5°C and warm-side cell temperature of 60°C, a pressure difference of about 10 bars is needed. Figure 6 illustrates a comparison between the pressure and the temperature difference needed to transport liquid water through the MEA (flooded configuration) at similar rates. These results indicate that temperature difference across the MEA generates significant driving force for water transport. Further experiments on bare Teflon-reinforced Nafion membrane (to simulate Gore-Select membrane) and also on an MEA (identical to what was used in the previous experiments) sandwiched between two untreated Toray papers in a flooded cell configuration showed the flow of water under the effect of temperature difference. These results indicate that temperature-driven water flow is a membrane-driven phenomenon, which agrees with studies reported on liquid water transport under the effect of temperature difference across other types of membranes.[18-20] This work is currently underway and will be discussed in a future publication. Also, based on these latter experiments, results from surface-tension calculations have indicated that surface tension changes due to temperature difference can generate a significant pressure difference across the membrane, which, based on estimated values of liquid water permeability,[16] can cause transport of water at rates comparable to what was experimentally measured in this work. Details of these findings will be published in another paper.

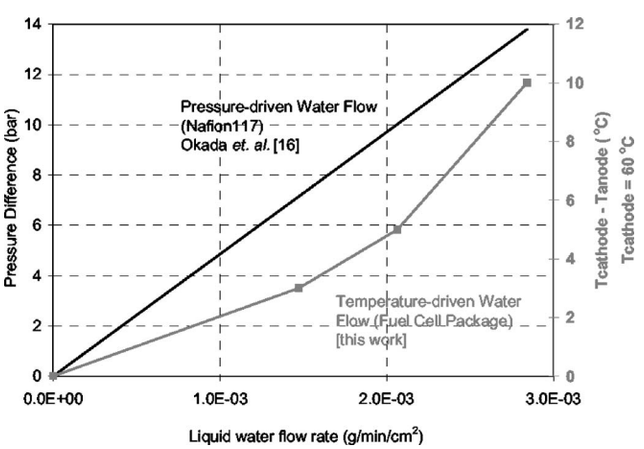

Figure 6. A comparison between temperature and pressure differences required for liquid water flow through the MEA (flooded configuration) at similar rates.

Conclusions

For the first time, an experimental examination has been performed to assess water transport through MEA during PEMFC operation under the influence of through-plane temperature difference. The study showed that during PEMFC operation, the presence of a temperature difference can force water to move across the membrane in the direction towards the colder side of the cell. The thermally driven water was shown to be significant when compared to the water generation rate at 0.4 A/cm^2. It was also found that increasing temperature and through-plane temperature difference in the cell causes an increase of water flow rate through the membrane. To provide more direct evidence of this water transport, the experiments were reconstructed to eliminate any other phenomena that may influence the water movement through the membrane by filling the gas compartments within the fuel cell apparatus used in the previous experiments with liquid water. With this simplified condition, thermally driven water flow was also observed showing trends similar to what was observed in the case of the fuel cell under operating conditions.

Findings from this work, though limited to a specific PEMFC design and components, highlight a new aspect of water transport in proton exchange membranes for fuel cells, that is, thermo-osmosis, thermally driven water transport. This suggests that transport physics of water through the membrane of an operating PEMFC have to be reconsidered in a more fundamental and comprehensive way by including thermo-osmosis. It also suggests the importance of including through-plane thermal profiles related to water management in designing PEMFC power systems.

Further experiments are needed to define the actual temperature and temperature difference that occurs across the membrane itself and to obtain a better understanding of the mechanism of thermo-osmosis in PEMFCs.

University of Connecticut assisted in meeting the publication costs of this article.

References

1. T. V. Nguyen and R. E. White, *J. Electrochem. Soc.*, **140**, 2178 (1993).
2. T. F. Fuller and J. Newman, *J. Electrochem. Soc.*, **140**, 1218 (1993).
3. R. Mosdale and S. Srinivasan, *Electrochim. Acta*, **40**, 413 (1995).
4. J. S. Yi, J. D. Yang, and C. King, *AIChE J.*, **50**, 2594 (2004).
5. P. Berg, K. Promislow, J. S. Pierre, J. Stumper, and B. Wetton, *J. Electrochem. Soc.*, **151**, A341 (2004).
6. J. S. Yi and C. King, UTC Fuel Cell Internal Memo (2001).
7. J. S. Yi and T. V. Nguyen, *J. Electrochem. Soc.*, **145**, 4 (1998).
8. T. Berning and N. Djilali, *J. Power Sources*, **124**, 440 (2003).
9. W. He, G. Lin, and T. V. Nguyen, *AIChE J.*, **49**, 3221 (2003).
10. R. Zaffou, J. S. Yi, and P. Hagans, Paper 1938 presented at The Electrochemical Society Meeting, Honolulu, HI, Oct 3–8, 2004.
11. C. Reiser, U.S. Pat. 5,700,595 (1997).
12. M. V. Williams, E. Begg, L. Bonville, H. R. Kunz, and J. M. Fenton, *J. Electrochem. Soc.*, **151**, A1173 (2004).
13. P. J. S. Vie and S. Kjelstrup, *Electrochim. Acta*, **49**, 1069 (2004).
14. W. Yan, F. Chen, H. Wu, C. Soong, and H. Chu, *J. Power Sources*, **129**, 127 (2004).
15. Y. Shan and S. Choe, *J. Power Sources*, **145**, 30 (2005).
16. T. F. Fuller and J. Newman, *J. Electrochem. Soc.*, **139**, 1332 (1992).
17. T. Okada, G. Xie, and M. Meeg, *Electrochim. Acta*, **43**, 2141 (1998).
18. M. Tasaka, S. Abe, S. Sugiura, and M. Nagasawa, *Biophys. Chem.*, **6**, 271 (1977).
19. M. Tasaka, T. T. Mizuta, and O. Sekiguchi, *J. Membr. Sci.*, **54**, 191 (1990).
20. F. Bellucci, *J. Membr. Sci.*, **9**, 285 (1981).